USGS
science for a changing world

U.S. DEPARTMENT OF THE INTERIOR
U.S. GEOLOGICAL SURVEY

PRELIMINARY SCIENTIFIC RESULTS OF THE CREEDE CALDERA CONTINENTAL SCIENTIFIC DRILLING PROGRAM

P.M. Bethke, Editor

Open-File Report 94-260-P

2001

GEOPHYSICAL LOGGING AND LOG PROCESSING BOREHOLES CCM-1 AND CCM-2, CREEDE, COLORADO

By

P. H. Nelson
J.E. Kibler
U.S. Geological Survey, Denver, CO

ABSTRACT

Geophysical logs were acquired in boreholes CCM-1 (Hosselkus 1-10) and CCM-2 (Airport 1-6) drilled into the Creede Formation and underlying volcanics immediately south and west of Creede, Colorado. Logs acquired include gamma ray, neutron, density, resistivity, sonic, and magnetic properties. Logging and data reduction procedures are briefly described. Geological and mineralogical data have been merged with the geophysical logs, and plots of the data are provided for each borehole.

INTRODUCTION

In support of the Creede drilling project, geophysical logs were acquired in two boreholes drilled into the moat of the Creede caldera during the autumn of 1991 (see Bethke, et al., Chapter A this report for hole locations). Logs were acquired with the USGS (Branch of Geophysics) logging truck, while the drilling and casing work was in progress. The logging tools are of the slimhole variety with diameters less than 2.5 inches. Each hole was logged in two stages, during which ten probes were run (see "description of logging equipment").

Data were acquired digitally using an IBM-compatible PC computer and stored on 3.5-inch disks. Digitization interval was 0.2 feet for most of the logs. In the office, the data were converted from measurement to physical units and corrections for hole size and other borehole effects were applied. Geological observations, stratigraphic picks, and mineralogical percentages from x-ray diffraction were acquired from other investigators and merged into the data set.

Here we describe the borehole measurements, give some details regarding data reduction, and present plots of the more important logs acquired at Creede. Discussion of the physical property variations revealed by the logs in terms of the stratigraphy is given by Larsen and Nelson (1994).

BOREHOLE CONDITIONS

Boreholes CCM-1 (Hosselkus 1-10) and CCM-2 (Airport 1-6) were logged in two stages. The upper section of each hole was logged just before surface casing was set through the gravels. The lower section was logged after the driller reached total depth. The reference point for logging was 30 inches above ground level for both holes.

Hole CCM-1 (upper). Conductor pipe was set to 22.5 feet. Hole diameter was 3.85 inches to a depth of 240 feet. The drilling mud contains bentonite and "drilleze" polymer with no barite. Drilling mud was circulated for about 45 minutes prior to logging. Liquid polymer was added towards the end of the circulation period. Chlorides in the makeup water were reported to be 350 ppm. The logging truck arrived on site at 9 pm on October 8, 1991 and logging commenced around midnight.

Hole CCM-1 (lower). Drill bit diameter was 3.85 inches to a total depth of 1371.5 feet. The driller circulated mud for 45 minutes before logging. Mike Buckley of Columbine Logging reported a mud resistivity (Rm) of 4.38 ohm-m at 67.7°F just one hour before logging. He said that Rm had been running between 3.25 to 4.5 ohm-m the last few days before logging. He measured 400 ppm Cl when the drillers depth was 1250 feet. He measured 5.09 ohm-m at 63.1 F about one hour after circulation stopped. The truck arrived on site at 11:45 pm on Friday, October 19, 1991. The drill rods were out of the hole at 2:45 pm on October 20 and logging commenced shortly afterwards.

Hole CCM-2 (upper). The hole was cased with 9 5/8 inch casing to 116 feet and with 4.5 inch (4.0 inch i.d.) casing to 139 feet. Bit diameter was 3.85 inches to 251 feet. The truck arrived on site at 1:30 pm on 30 October, 1991. Logging commenced at 1:30 am on 31 October.

Hole CCM-2 (lower). Hole was cased to 254 feet and drilled to 2323 feet with a 3.85 inch bit. Flow was reported from the vicinity of 1700 feet at 40 gpm with resistivity of 16 ohm-m and 310 ppm Cl. Mud weight was 8.8 pounds per gallon and viscosity was 70. The truck arrived on site at 7 pm and logging commenced around 9 pm on November 14, 1991.

DESCRIPTION OF LOGGING EQUIPMENT

Ten probes were operated from the USGS logging truck. The complex resistivity probe also required mobilization of a second van containing computer equipment required by that probe. A brief description of each probe follows. An individual probe may produce anywhere from one to six logs or curves. Curves for each probe are listed in Appendix A.

Depth and depth shifts

Data were acquired at a depth spacing of 0.2 feet, with the exceptions of magnetometer (roughly 0.5 feet) and complex resistivity data (2.0 feet). Office processing consisted of elimination of occasional erroneous entry of depth and signals, elimination of data recorded where the probe was stopped, and elimination of overlapping segments. The depth was corrected to ground level by subtracting 2.5 feet from the recorded depth. Subsequent depth corrections were done with interactive computer software, first depth shifting the 8-inch resistivity and susceptibility logs to lithologic contacts, then shifting the magnetometer log to the susceptibility log and shifting all other logs to the 8-inch resistivity log. After removal of the 2.5 foot correction, subsequent shifts were generally about one or two feet.

Caliper/temperature/fluid resistivity

This probe uses an upper section to measure hole diameter and a lower section to measure the temperature and resistivity of the borehole fluid. The caliper section contains 3 spring-loaded arms with motor drive for opening and closing the arms. Calibration is performed with a set of three rings of known diameter.

This probe was the first to be run. Temperature and fluid resistivity were recorded going into the hole, then the arms opened while the probe was at bottom, and a caliper log recorded coming out of the hole. The temperature logs show a break between the upper and lower runs (near 250 feet in figure 1) due to changes in temperature of the drilling fluid at the time of logging. Changes in slope are due to fluid loss or entry (1100 to 1350 feet in CCM-1, figure 1). The temperature offset at 860 feet in CCM-2 is attributed to heavy mud emplaced to stabilize the borehole. Note that the Rm values at the bottom of CCM-1 and CCM-2 are quite comparable with the values of 5 and 16 ohm-m reported under the section "borehole conditions".

Drift

The drift or directional survey probe contains a magnetic compass to measure orientation and two inclinometers to measure inclination from the vertical. The system is used to make directional surveys in boreholes inclined up to 25° from the vertical in open holes. Because the compass is magnetic, the probe will not function within or near iron casing, and the survey will be incorrect in rocks having a high magnetization.

Measurements of inclination in CCM-1 showed the hole to be within 1 degree of vertical to total depth. Consequently, the depth recorded with the logs in CCM-1 is equivalent to vertical depth below surface.

In CCM-2, the drift tool measured an inclination of 5 degrees off vertical at the bottom of the upper section (250 feet). The drift tool was mysteriously lost after this run, and was never found. However, the inclinometers in the magnetic field tool measured an inclination of approximately 5 degrees to the bottom of the hole. Consequently, the true vertical depth is slightly shallower (0.4%) than the depth recorded with the logs: a measured depth of 1000 feet corresponds to a true vertical depth of 996.2 feet.

Density

The Mt. Sopris dual density probe contains two collimated CsI (Na) scintillation detectors spaced 20.7 cm and 35.2 cm from a 100mCi Cs-137 source. A single caliper arm located above the two detectors is used to press the source and detectors against the borehole wall. The count rate data from the two detectors are used to determine bulk density. Calibration is performed using an aluminum and a plexiglass block of known density.

Gamma Ray/Neutron

The Comprobe gamma-ray/neutron probe contains a gamma-ray detector and a neutron-thermal neutron section. The total-count gamma ray measurement utilizes a NaI-photomultiplier detector. The output, in API gamma ray units, is useful for lithologic identification and stratigraphic correlation. Located in the lower part of the tool, the neutron probe detects thermal neutrons utilizing a He-3 detector spaced 16 inches (40.6 cm) from an Am-Be source (3.0 Ci Am-241). The neutron output is scaled to a porosity index.

Resistivity

The 4-channel resistivity module provides a 6 Hz constant-current source and four voltage channels. The primary current electrode is at the bottom of the tool, and voltage pickup electrodes are spaced 8, 16, 32, and 64 inches above the current electrode. The voltage and current readings are combined with a geometric factor to produce an apparent resistivity for each electrode. Apparent resistivity is corrected for hole diameter and mud resistivity effects by use of a caliper log and fluid resistivity measurements.

The point resistance curve (RPT) is simply the ratio of voltage to current (times a constant) at the primary current electrode. Its vertical resolution, on the order of several inches, is the best of all the logs, except the caliper.

Magnetometer

The 3-component magnetometer probe is described in detail by Scott and Olson (1985). The probe's gyroscopic azimuthal reference was not working at Creede, so directional information was not obtained with this tool. The three orthogonally oriented fluxgate magnetometer elements measure the Earth's magnetic field to a resolution of 10 nanoTeslas (nT) over a range from -80,000 to +80,000 nT. The magnetometer results are used for detecting strongly magnetized volcanic rocks and for detecting anomalies caused by concentrations of strongly magnetized ferromagnetic minerals.

Magnetic Susceptibility

The magnetic susceptibility probe (Scott and others, 1981) contains a sensing coil 12 inches long. The amplitude of the susceptibility signal is a nearly linear function of the susceptibility of rock near the borehole in the range 0-20,000 x 10^{-6}cgs. The conductivity signal is useful only for detecting concentrations of highly conductive minerals such as graphite and metallic sulfides because at the operating frequency of 1000 Hz the bridge is relatively insensitive to changes in resistivity above 0.1 ohm-meter. Tool output is in cgs or SI units with a range of 10^{-5} to 10^{-1} cgs (10^{-4} to 10^{0} SI). Results are used for detecting high susceptibility anomalies caused by concentrations of ferromagnetic minerals, and low susceptibility anomalies caused by alteration of ferromagnetic minerals.

Due to an electronics problem, we found that the gain of the susceptibility channel was not linear during the logging at Creede. To correct for this non-linearity, the susceptibility log was compared with core measurements provided by J. Rosenbaum and R. Reynolds (written comm., 1992). A quadratic fit of core to log data provided an adequate correction. A comparison of the corrected log and the core data is shown in figure 2.

Sonic

The Mt. Sopris sonic probe digitizes two received waveforms downhole which are used to determine the compressional wave transit time. The operator must manipulate the gains to achieve a stable transit time log. The outputs consist of

interval transit time (microseconds/ft) of P-wave (first arrival) between selected pair of receivers and the relative amplitude of first-arrival energy. The interval transit time is used to determine P-wave velocity of the formation and to estimate porosity; amplitude is used to detect fracturing and other sources of attenuation.

The sonic travel time (deltatus) trace has been edited to eliminate erroneous data caused by cycle skips. Missing data are particularly noticeable in the bottom of CCM-2.

Temperature

A high-resolution temperature probe was run after the preceding logs and before the complex resistivity probe. The purpose of acquiring a second temperature log was to measure the temperature of the borehole fluid about 12 hours after mud circulation. When this probe was run, insufficient analog gain resulted in visible discrete steps in the resulting temperature log. Even after some smoothing, the log still has a noisy appearance (compare TEMPPT_C with TEMP_C in figure 1).

Complex Resistivity

The complex resistivity equipment (Olhoeft and Scott, 1980) applies a 1 Hz sine wave to the current electrode of a 16-inch normal probe. The received voltage is analyzed for amplitude, which is converted to apparent resistivity, phase shift, which is a measure of the induced polarization, and total harmonic distortion of the first through third harmonics.

GEOLOGICAL AND MINERALOGICAL DATA

The lithologic units presented by Hulen (1992) were entered into the data set and presented with plots distributed previously to project investigators. The lithologic descriptions and boundaries subsequently refined by Larsen (Larsen and Nelson, 1994) are used here in figures 3 and 4. Both sets of lithologic boundaries are stored in the data base (Appendix A).

X-ray diffraction data were supplied to us by Dave Finkelstein for the minerals listed in Table 1, as weight percent of total solids. These percentages were combined with calculated mineral density values from Ellis et al (1988) to compute grain density values. The chemical formulae and mineral density values are given in Table 1.

PRESENTATION OF DATA

It is not practical to present all the processed curves listed in Table A1, so curves judged to be the most important are presented in figures 3 and 4. Lithology and grain size estimates are shown in column 1; mineralogy is shown in column 2. Core run numbers are given at the right edge of the depth column.

Columns 3-7 contain the geophysical logs. Gaps in the logs at 240-250 feet occur at the bottom of the upper logged sections (see section "borehole conditions"). The caliper shows that borehole openings are few in number and only a fraction of an inch in extent; thus the other measurements are free of spurious effects due to

changes in borehole diameter. The neutron, density, resistivity, and sonic traces all respond to changes in porosity and clay/clinoptilolite content. Increases in porosity and/or clay content cause deflections to the left. The magnetic field log mainly responds to changes in remanent magnetization within the volcanics.

The following comments highlight some log responses that can be seen in figures 3 and 4 and that require explanation in terms of lithological, mineralogical, or even chemical influences. A detailed discussion of the log response in terms of lithology is being presented separately (Larsen and Nelson, 1994).

1. At 1203 feet in CCM-1, and at 1606 feet in CCM-2, most physical properties change in response to an increase in porosity as the logs pass from the volcanic breccias into the sediments. The resistivity log is particularly effective at distinguishing among the different types of breccia in CCM-1. However, the change in level of magnetic susceptibility is not coincident with the volcanic/sedimentary boundary.

2. The graded tuff beds extending from 1128 to 1203 feet in CCM-1 and from 2000 to 2038 feet in CCM-2 produce monotonic increases with depth in the neutron, density, resistivity, and sonic logs. These slopes are attributed to decreases in sorting as grain size increases with depth. Also note the coincident linear increases in magnetic susceptibility.

3. The fall-out tuffs usually produce decreases in resistivity and density and increases in neutron porosity, with respect to the lacustrine strata. However, tuffs D4 and F in CCM-1 produce resistivity increases. Mineralogically, these two tuffs differ from others in CCM-1 by their high (40-50%) quartz content, higher (30%) K-feldspar content, low clay, and zero clinoptilolite content.

4. Although resistivity is low in the clinoptilolite-rich fallout tuff beds in CCM-2, there is no response in either the total harmonic distortion or the induced polarization curves. Instead, enhanced distortion and polarization occur sporadically in the volcanic units. Similarly in CCM-1, significant increases in total harmonic distortion (_10%) occur in ash-flow tuffs and in the debris-flow strata.

5. Although not easily discerned on the plotting scale used in figures 3 and 4, the density, neutron, and sonic logs all exhibit trends of decreasing porosity with increasing depth in the fallout tuffs and lacustrine strata which can be attributed to a compaction gradient. However the resistivity logs do not have such a simple monotonic gradient. In CCM-1, the interval from 440 to 645 feet is characterized by low resistivity and increased harmonic distortion. And in CCM-2 the resistivity log is unchanging over the interval 820-1220 feet and decreases with depth from 1220 to 1605 feet.

ACKNOWLEDGEMENTS

C. Stoddard operated the USGS logging truck and D. Capron acquired and processed the complex resistivity logs, with assistance from F. Clutsom, J. Lucius, and J. West. Mineralogical data were provided by D. Finkelstein of the University of Illinois. Lithologic data were provided by D. Larsen of the University of New Mexico.

REFERENCES

Ellis, D., Flaum, C., McKeon, D., Scott, H., Serra, O., and Simmons, G., 1988, Mineral Logging Parameters: Nuclear and Acoustic: The Technical Review, v.36, n.1, p. 38-52; *reprinted in* Formation Evaluation I, AAPG Treatise of Petroleum Geology Reprint Series No. 16, American Association of Petroleum Geologists, 1990, p. 460-474.

Hulen, J.B., 1992, Field geologic log summaries (1 in. = 12 ft.) for Coreholes CCM-2 (Airport 1-6) and CCM-1 (Hosselkus 1-10), University of Utah Research Institute, DOE/ER/14207-1, ESL-92001-TR, 40 p.

Scott, J.H., Seeley, R.L., and Barth, J.J., 1981, A magnetic susceptibility well-logging system for mineral exploration, paper CC in Trans. of 22nd Annual Logging Symposium, Society of Prof. Well Log Analysts, 21 p.

Scott, J.H. and Olson, 1986, Development of a 3-component borehole magnetometer probe with gyroscopic orientation, in Borehole Geophysics for Mining and Geotechnical Applications, ed. P.G. Killeen, Geol. Survey of Canada, Paper 85-27.

Olhoeft, G.R., and Scott, J.H., 1980, Nonlinear complex resistivity logging, paper T in Transactions of 21st Annual Logging Symposium, Society of Professional Well Log Analysts, 18 p.

Table 1. Chemical formulae and density values for selected minerals from Ellis et al. (1988).

Name	Chemical Formula	Density (g/cm^3)
Clays --		2.50
Montmorillonite	$Na_{.3}(Al_{1.67}Mg_{.33})(Si_4O_{10})(OH)_2$	
Illite	$K_{.8}(Al_{1.6}Mg_{.2}Fe_{.2})(Si_{3.4}Al_{.6})O_{10}$	
Kaolinite	$(OH)_2$	
	$Al_4(Si_4O_{10})(OH)_8$	
Quartz	SiO_2	2.65
Sanidine	$KAlSi_3O_8$	2.57
Authigenic Kspar	$KAlSi_3O_8$	2.57
Plagioclase	$NaAlSi_3O_8$, $CaAl_2Si_2O_8$	2.64
Calcite	$CaCO_3$	2.71
Biotite	$K(Mg,Fe)_3(AlSi_3O_{10})(OH)_2$	3.22
Pyrite	FeS_2	5.01
Clinoptilolite	$(K_2,Na_2)(Al_2Si_7O_{18})\_6H_2O$	2.20
Analcime	$Na(AlSi_2O_6)\_H_2O$	2.28
Opal-CT	SiO_2	2.32
Amphibole	$Ca_2Fe_5(Si_8O_{22})(OH)_2$	3.44

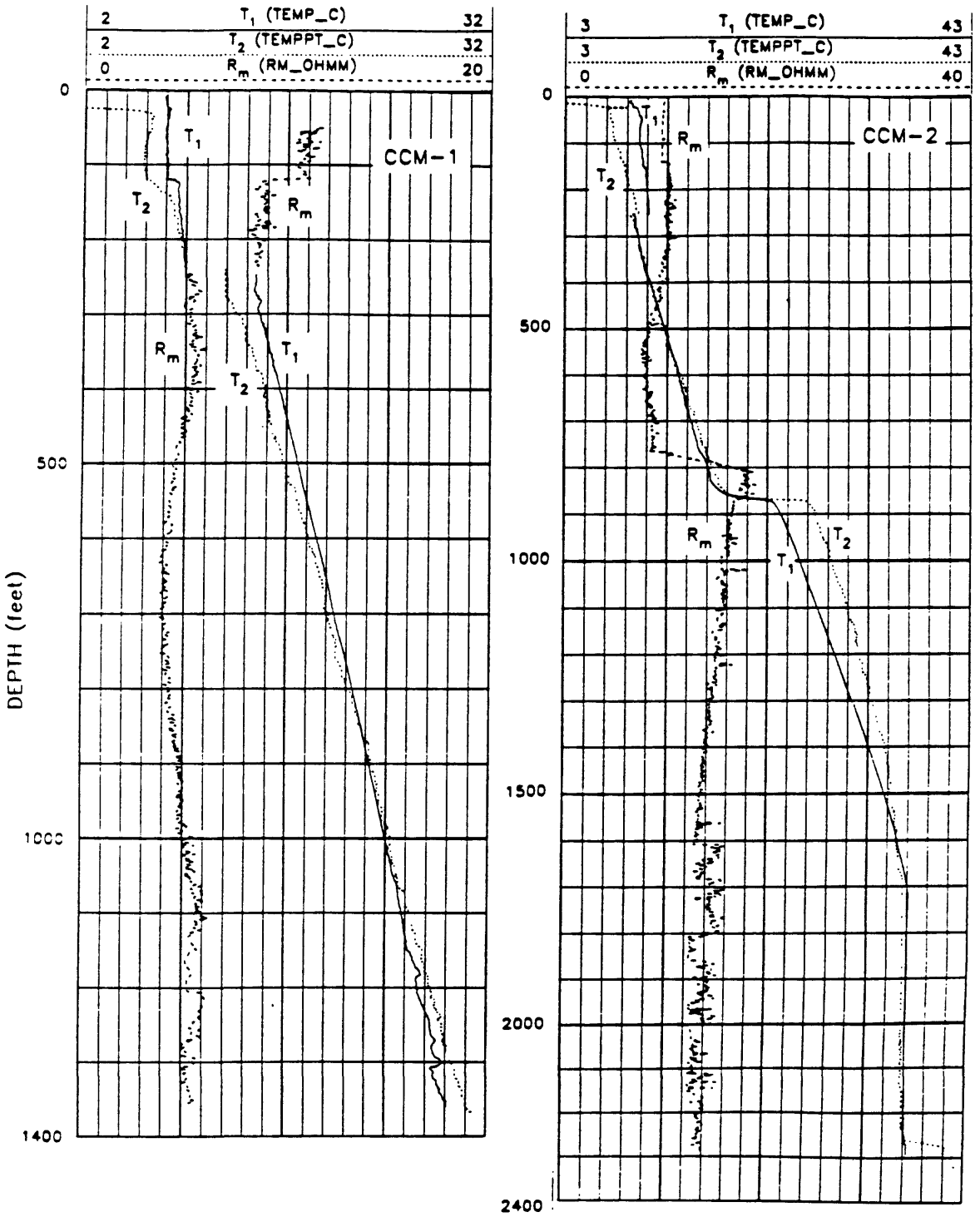

Figure 1. Temperature and fluid resistivity logs in boreholes CCM-1 and CCM-2, all recorded on down-going runs. Temperature log T1 was generally recorded within one to two hours after cessation of drilling fluid circulation. Temperature log T2 was recorded about 12 hours after log T1. Inadequate recording resolution contributes to the noisy appearance of log T2. Fluid resistivity Rm decreases as temperature increases.

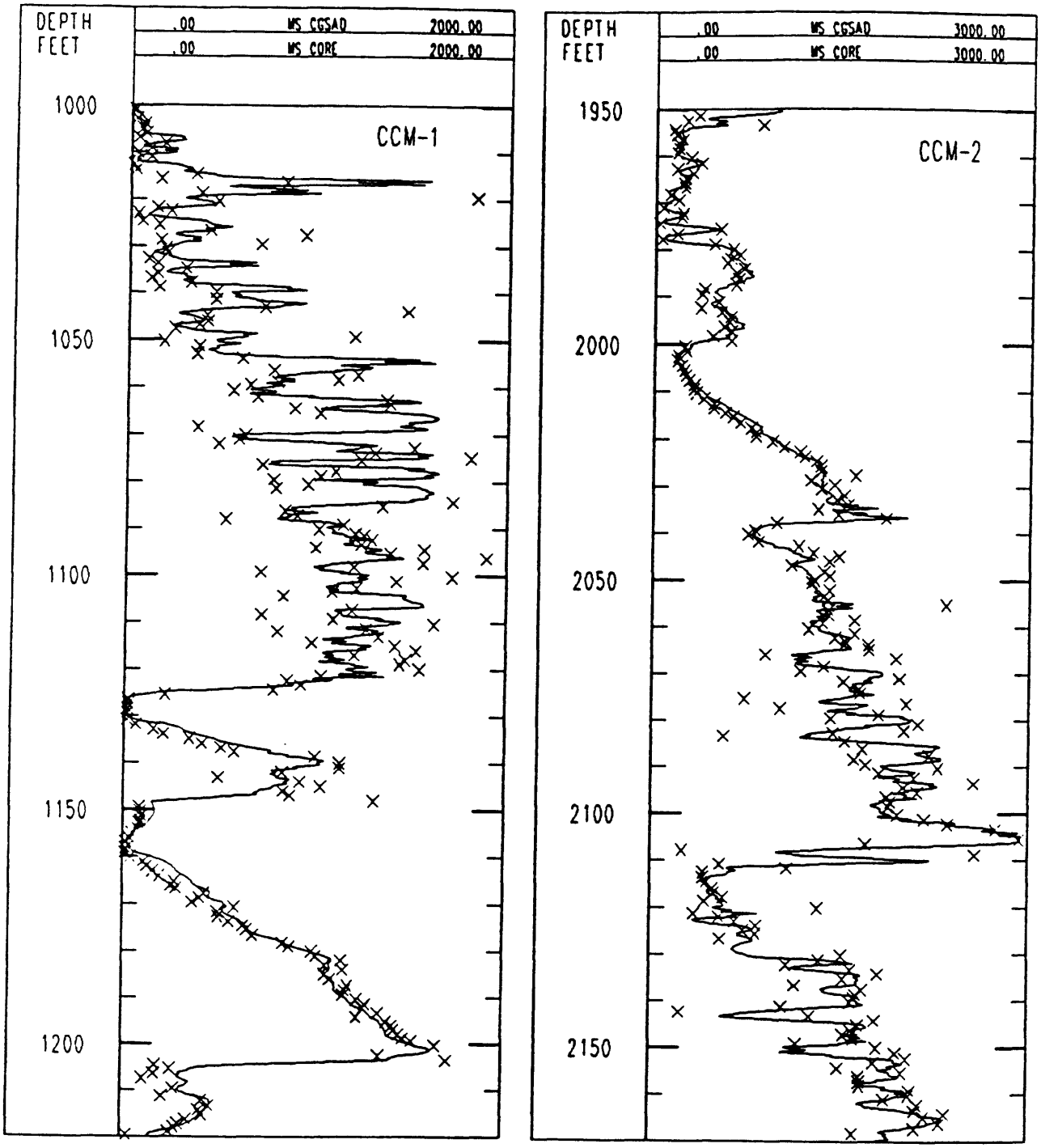

Figure 2. Comparison of magnetic susceptibility core data (X) and logs (solid line), in micro-cgs units. The logs have been corrected to the core data.

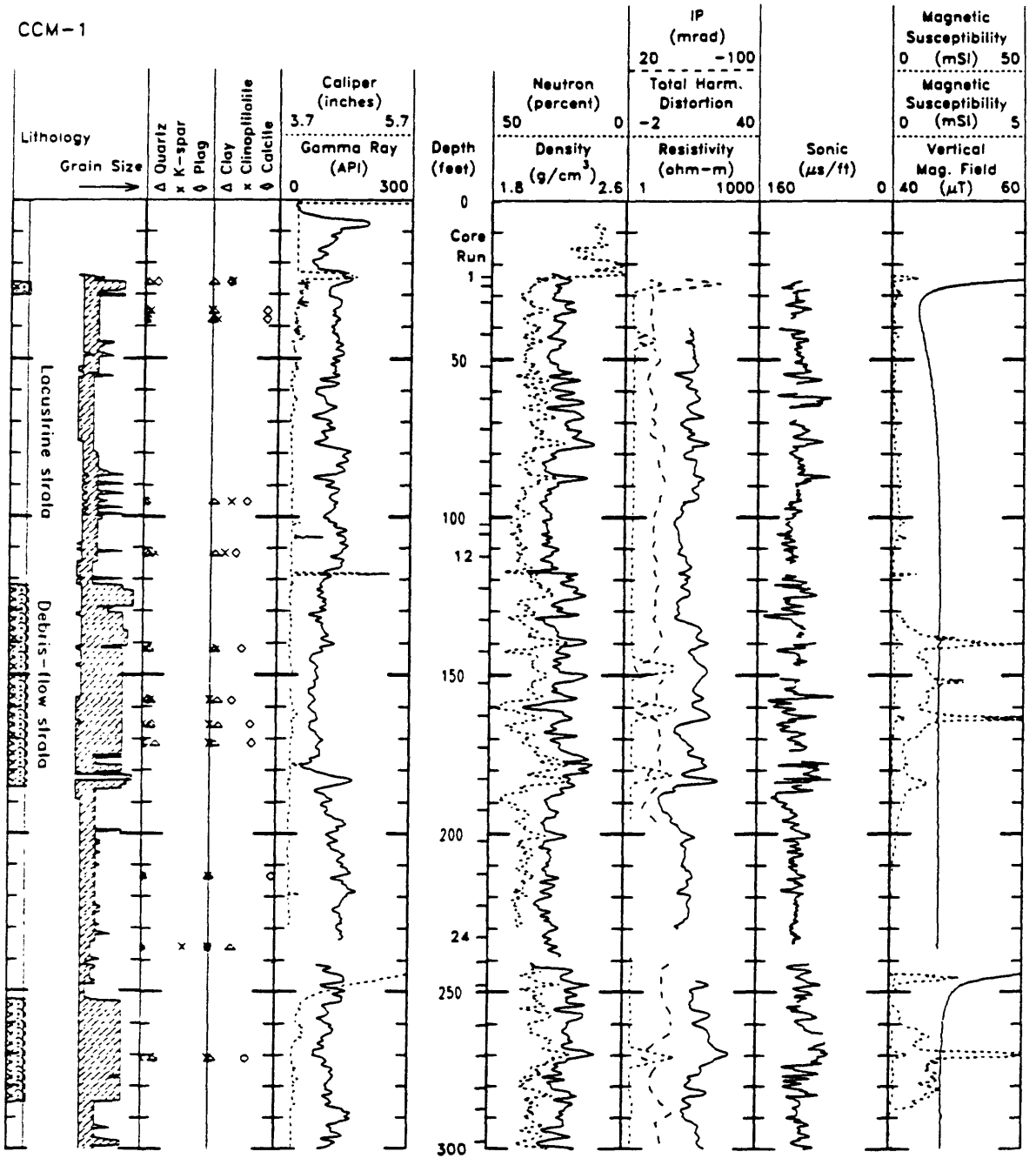

Figure 3. Representive logs from borehole CCM-1. Core runs are indicated on the right side of the depth column. Curve names are explained and units given in Appendix A. Column 1: Lithology from Larson and grain size from Hulen. 2: Mineral content by x-ray diffraction from Finklestein. 3: Caliper, CAL_INCH, and gamma ray, GR_API. 4: Neutron porosity (total water content), NEU_POR, and bulk density, RHOB. 5: Resistivity, R08_RM, phase angle, IP_CR, and total harmonic distortion. 6: Sonic travel time, DELTATUS. 7: Vertical magnetic field, ZD and magnetic susceptibility MS_SIADJ. Susceptibility is presented on an amplified scale for the upper section of the hole.

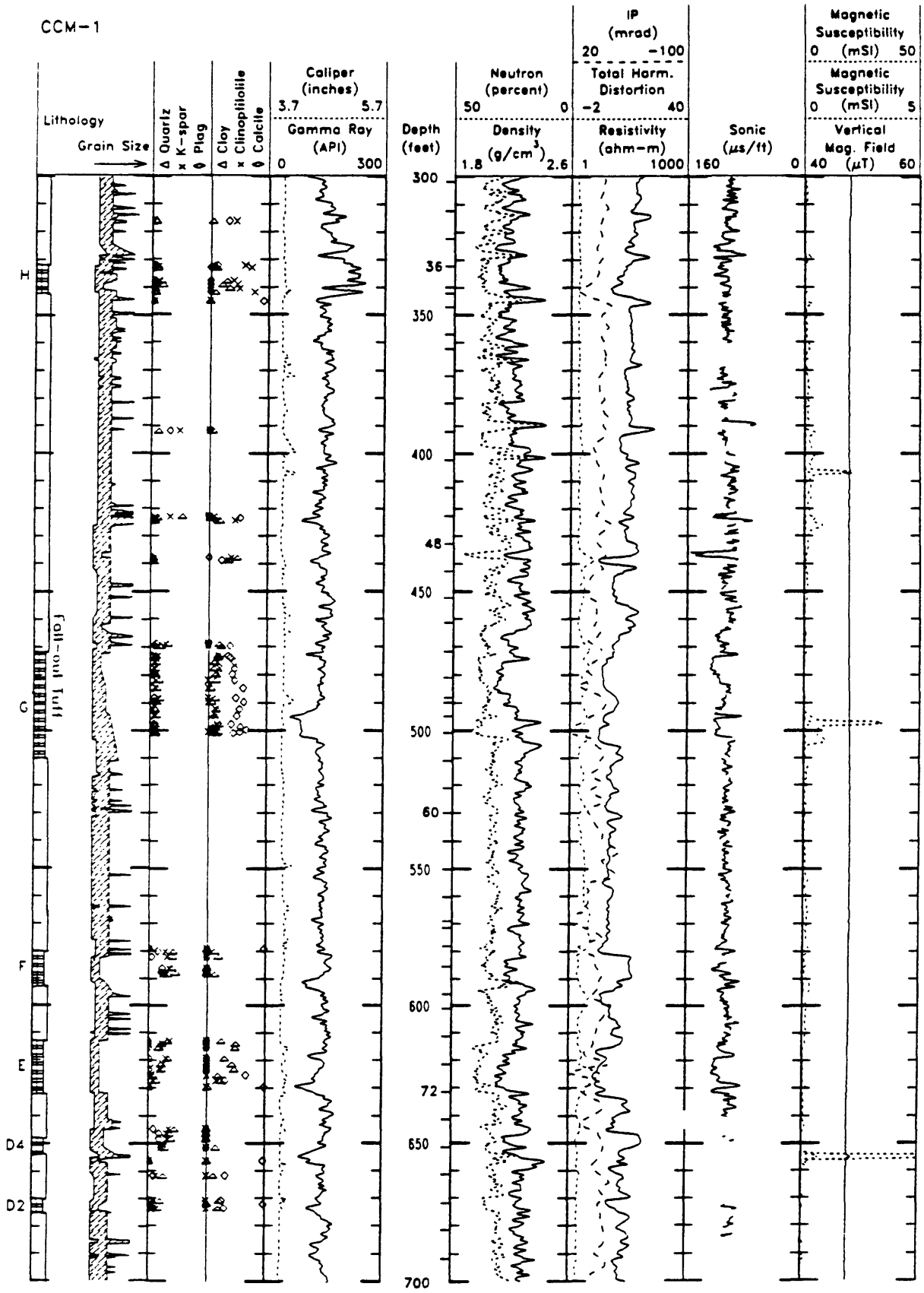

Figure 3, continued.

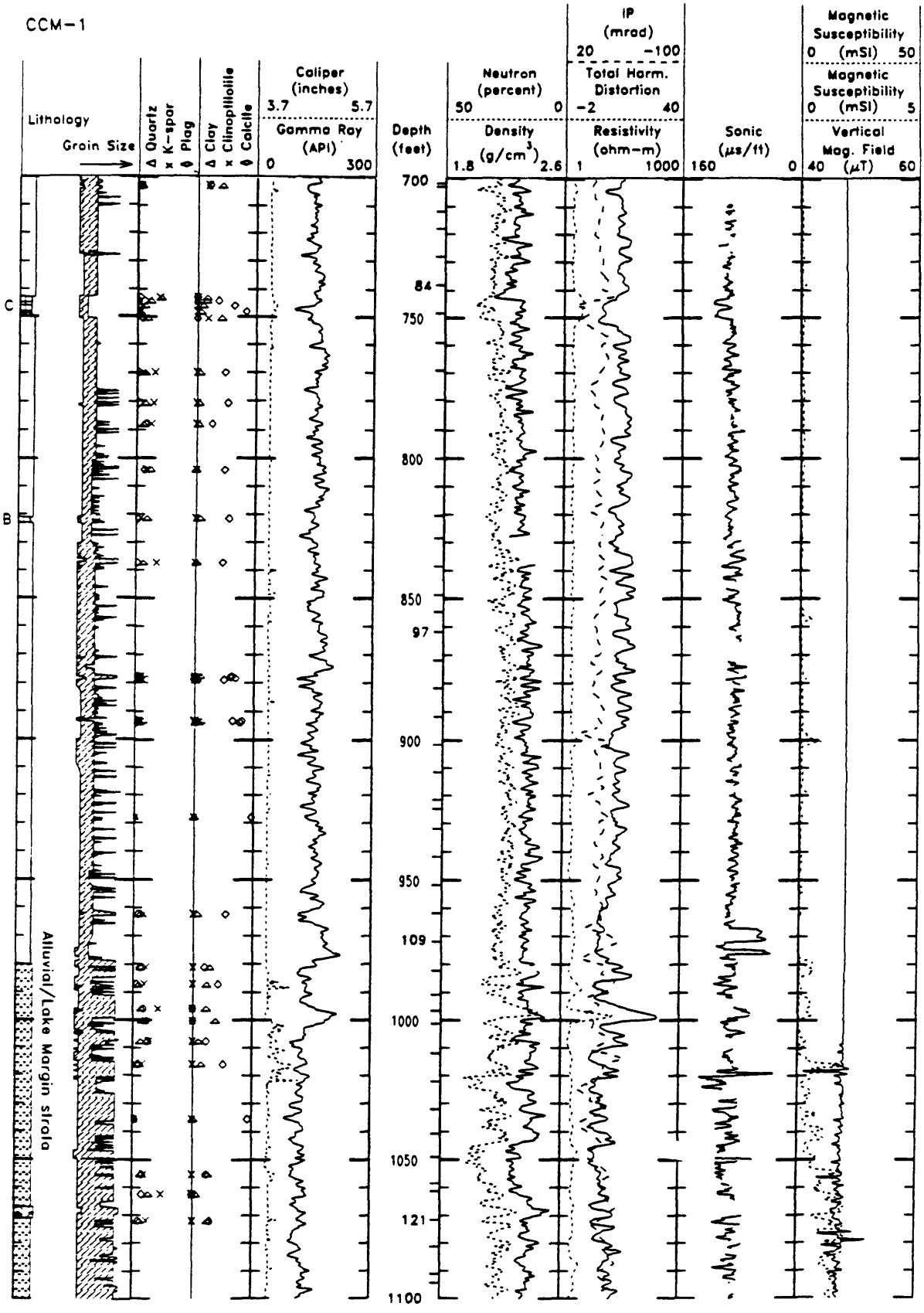

Figure 3, continued.

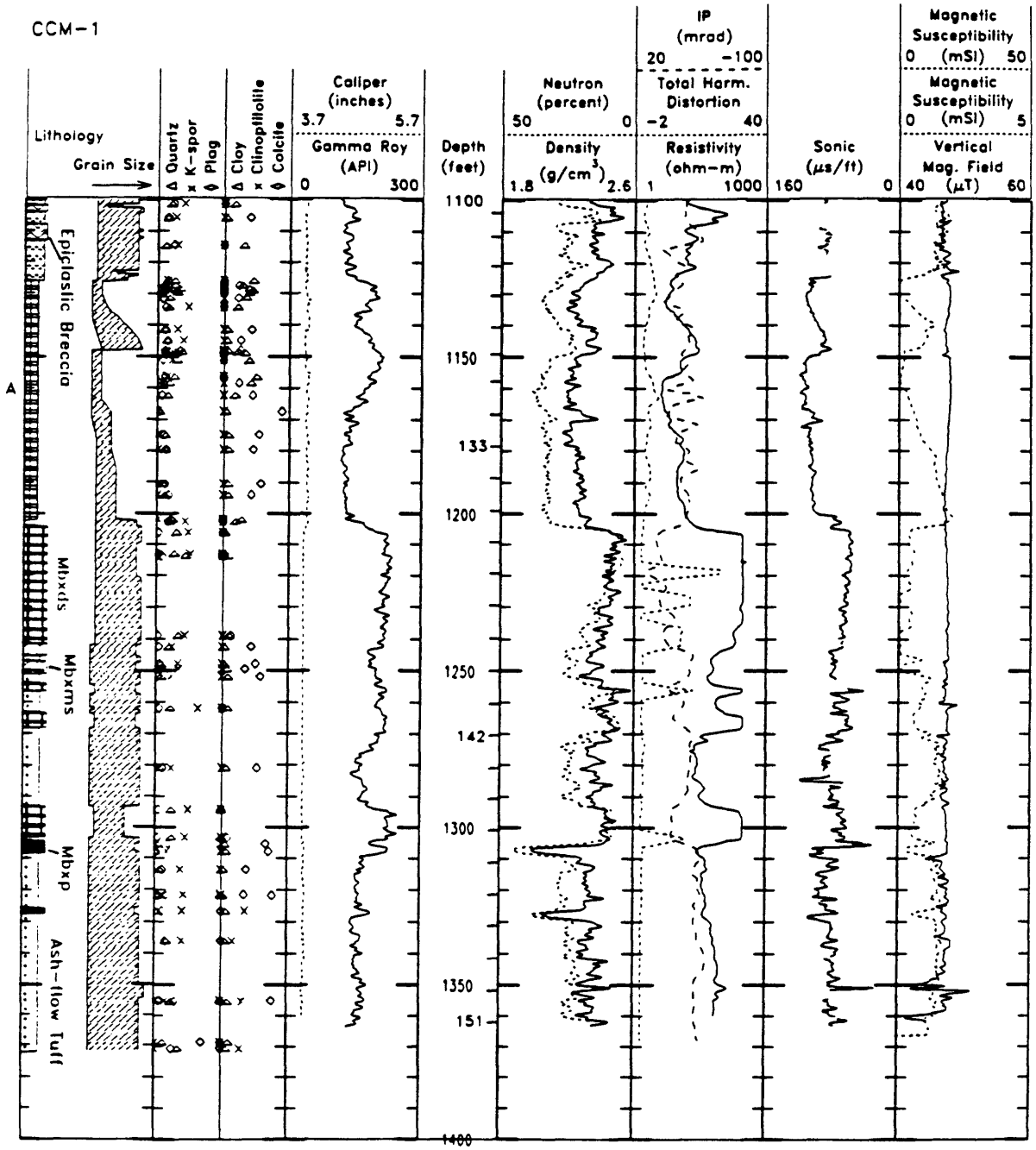

Figure 3, continued. Mbxp, Mbxms, Mbxds are porous, moderately silicified, and densely silicified megabreccias.

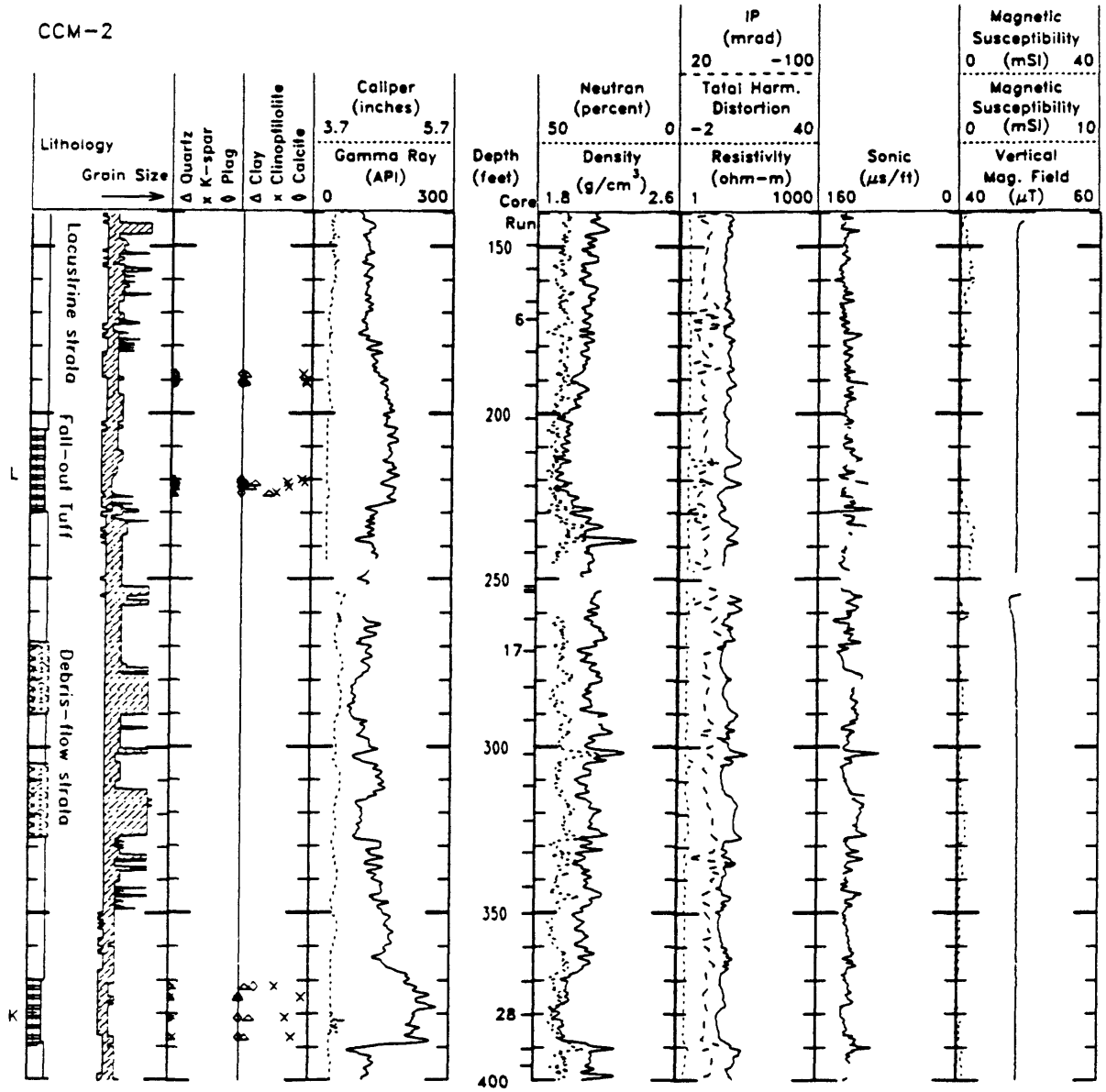

Figure 4. Representive logs from borehole CCM-2. Core runs are indicated on the right side of the depth column. Curve names are explained in Appen[illegible] Column 1: Lithology from Larson and grain size from Hulen. 2: Mineral content by x-ray diffraction from Finklestein. 3: Caliper, CAL_INCH, and gamma ray, GR_API. 4: Neutron porosity (total water content), NEU_POR, and bulk density, RHOB. 5: Resistivity, R08_RM, phase angle, IP_CR, and total harmonic distortion. 6: Sonic travel time, DELTATUS, and fractured interval. 7: Vertical magnetic field, ZD and magnetic susceptibility MS_SIADJ. Susceptibility is presented on an amplified scale for the upper section of the hole.

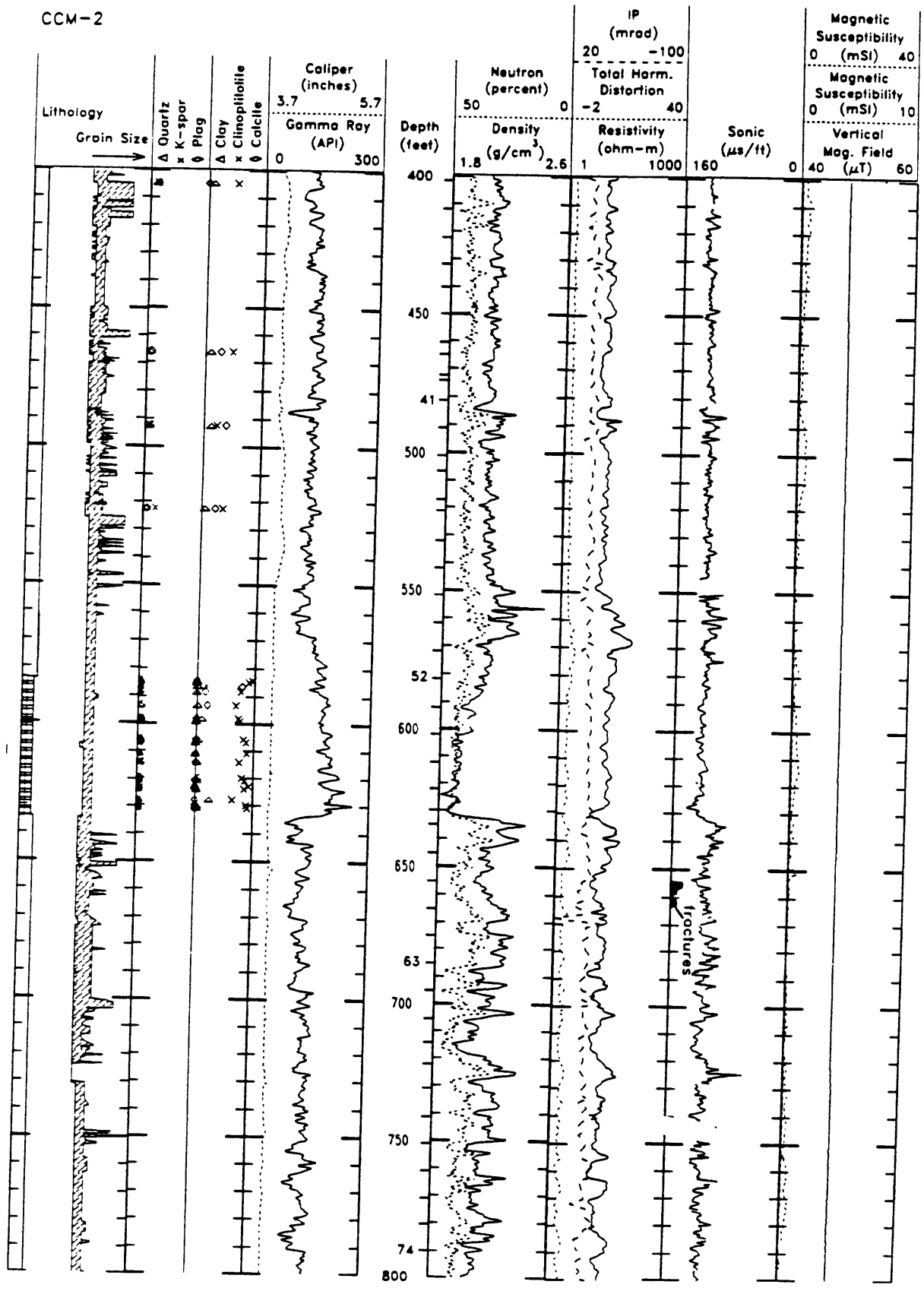

Figure 4, continued.

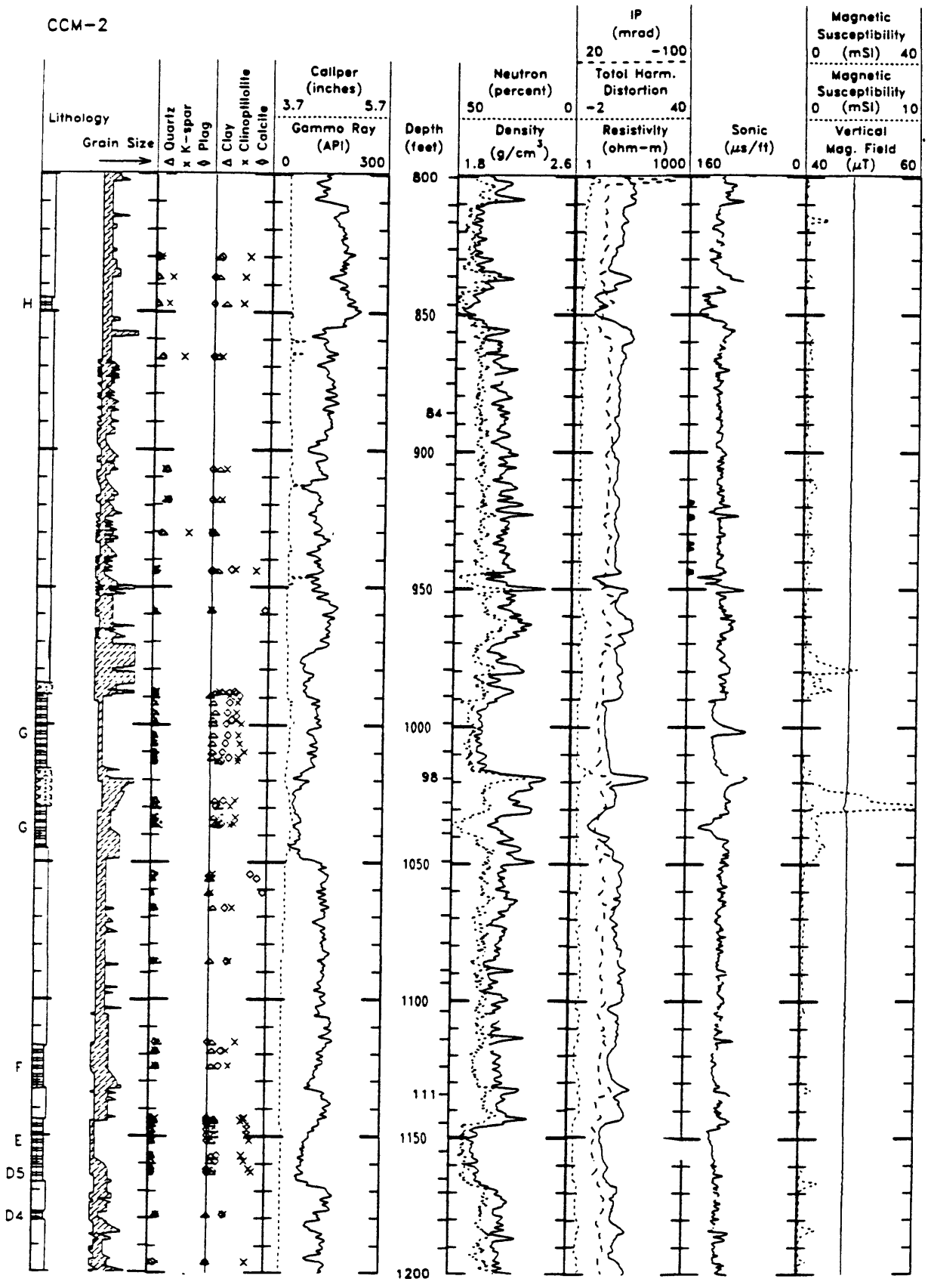

Figure 4, continued.

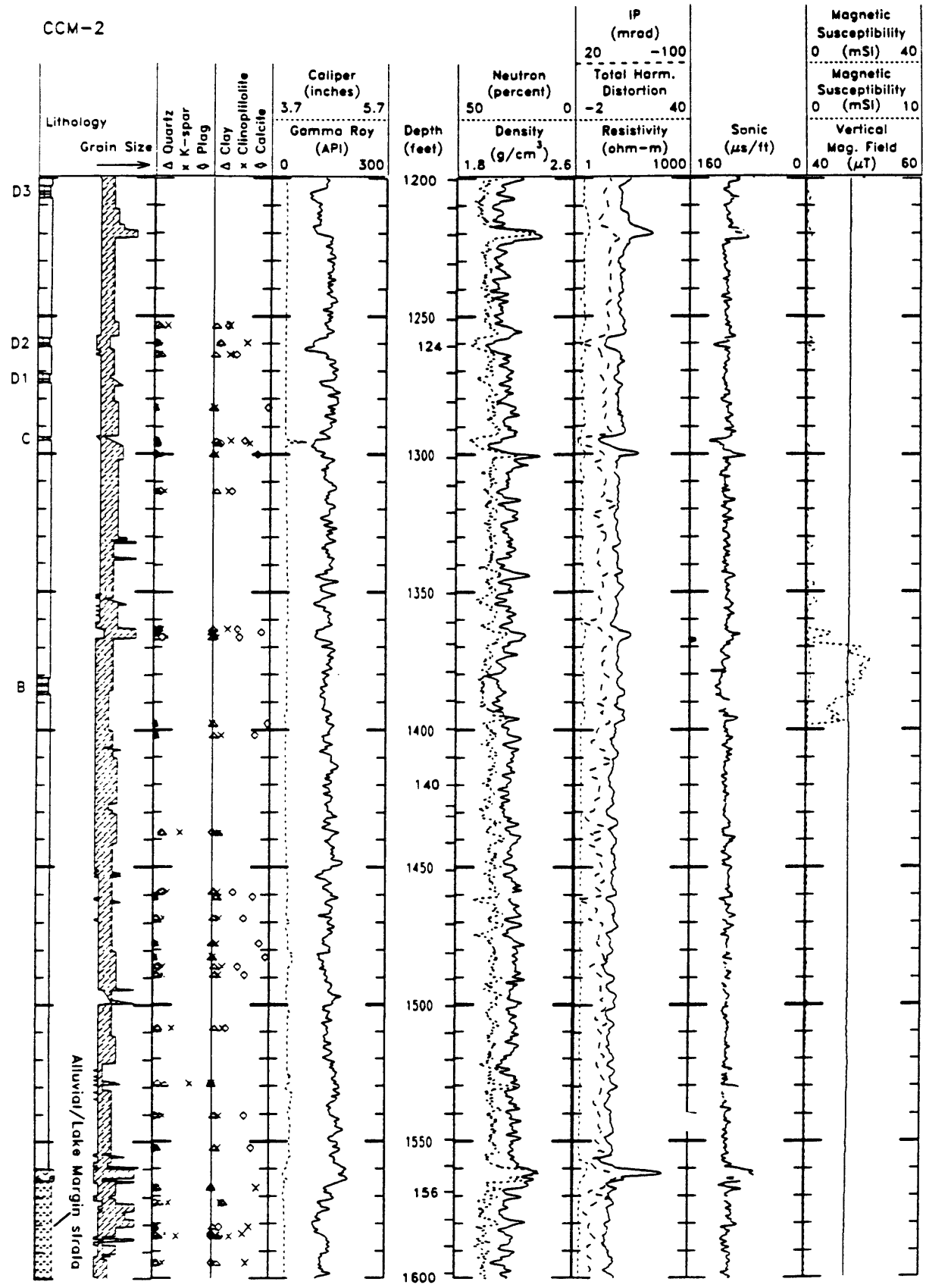

Figure 4, continued.

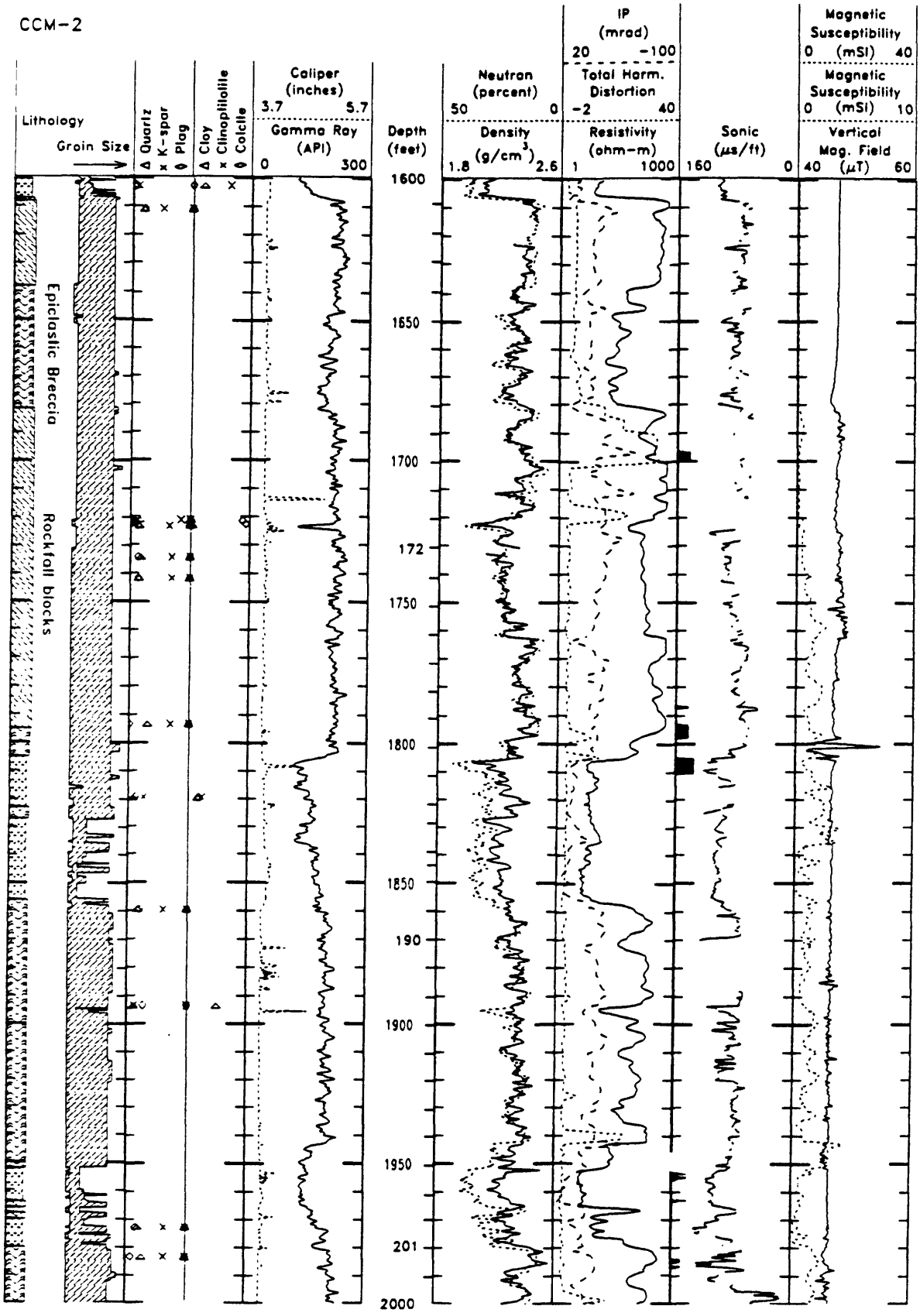

Figure 4, continued.

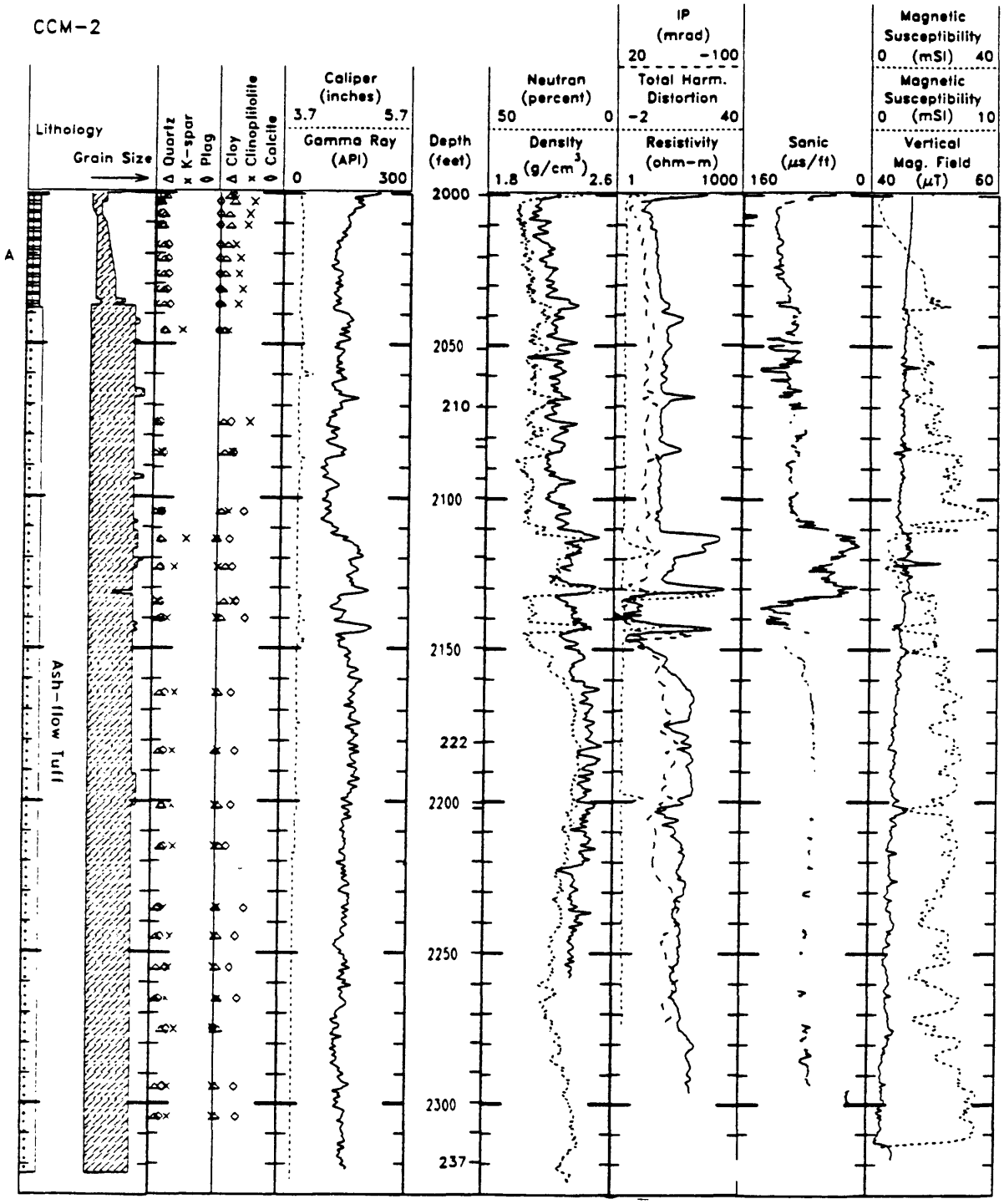

Figure 4, continued.

APPENDIX A. Data base for geophysical logs, core, and stratigraphic intervals.

Logs, core data, and geological information are stored using a software package designed specifically for borehole data. Data from CCM-1 and CCM-2 are each stored in a "well" consisting of up to 150 curves. All curves must be stored at the same spatial density, selected to be five points per foot for the Creede data. Intervals of 'no data' are stored as null values, as are all points between measurements in a curve of core data or a curve of stratigraphic tops. The software recognizes null values as points not to be computed or plotted.

Both the original logs and processed logs are stored in the data base. For example, CAL_MV is the original caliper log recorded in millivolts (after editing of overlapping intervals) and CAL_INCH is the processed log giving the borehole diameter in units of inches.

Table A1. List of geophysical logs and core measurements stored as curves in data base, five points per foot of borehole.

No.	Name	Descriptor	Units
1.	DEPTH	Depth	
135.	CORE_RUN	Tops of core runs	ticks
Caliper - Temperature - Resistivity			
4.	CAL_MV	Caliper	mV
5.	TEMP_MV	Temperature	mV
6.	RM_MV	Fluid resistivity	mV
56.	CAL_INCH	Caliper	inch
57.	TEMP_C	Temperature	deg C
58.	DTEMP_C	Differential temperature	deg C/km
59.	RM_OHMM	Fluid resistivity	ohm m
Resistivity			
8.	R08_MV	8-inch normal	mV
9.	R16_MV	16-inch normal	mV
10.	R32_MV	32-inch normal	mV
11.	R64_MV	64-inch normal	mV
12.	VXMTR	transmitter voltage	mV
13.	IXMTR	transmitter current	mV
61.	R08_OHMM	8-inch normal	ohm m
62.	R16_OHMM	16-inch normal	ohm m

63.	R32_OHMM	32-inch normal	ohm m
64.	R64_OHMM	64-inch normal	ohm m
65.	RPT	Point resistance	ohm
66.	R08_RM	8-inch normal	ohm m
67.	R16_RM	16-inch normal	ohm m
68.	R32_RM	32-inch normal	ohm m
69.	R64_RM	64-inch normal	ohm m

Gamma Ray/Neutron

19.	GR_CPS	Gamma ray	cps
20.	NEU_CPS	Thermal neutron	cps
77.	GR_API	Gamma-ray	api
78.	NEU_POR	Neutron porosity	percent

Density

21.	CALDD_MV	Caliper	mV
22.	NEAR_CPS	Near detector	cps
23.	FAR_CPS	Far detector	cps
79.	CALDD_IN	Caliper, inches	inch
80.	NEAR_GCC	Density, near det.	g/cc
81.	FAR_GCC	Density, far det.	g/cc
82.	RHOB	Density, compensated	g/cc
83.	COMP	Compensation, g/cc	g/cc

Sonic

24.	DELTAT	Delta-t	mV
25.	AMPFAR	Amplitude, far rcvr	mV
26.	AMPRATIO	Amplitude ratio	mV
43.	DELTATED	Delta-t, edited	us/ft
85.	DELTATUS	Delta-t, microsec/foot	us/ft
86.	PVEL_M/S	Sonic velocity	m/s

Magnetic Susceptibility

27.	MS_MV	Magnetic susceptibility	mV
28.	COND_MV	Conductivity	mV
29.	TEMPMS_M	Tool temperature	mV
87.	MS_CGS	Mag. susceptibility, cgs	ucgs
88.	MS_SI	Mag. susceptibility, SI	uSI
89.	COND_SCL	Conductivity, scaled	
136.	MS_SIUP	Mag. susc, upper sections	uSI
141.	MS_SIADJ	Mag. susc, adjusted to core	uSI
142.	MS_CGSAD	Mag. susc, adjusted to core	ucgs

Magnetometer

31.	XM	X-magnetometer	mag
32.	YM	Y-magnetometer	mag
33.	ZM	Z-magnetometer	mag
35.	XI	X-inclinometer	mag
36	YI	Y-inclinometer	mag
37	TEMPMAG	Tool temperature	mag
38	PTEST	Power supply dev.	mag
39.	INCOWL	Inclination fm Owl module	mag
40.	AZOWL	Azimuth fm Owl module	mag
92.	ZD	Vertical magnetic comp.	mag
93.	HM	Horizontal magnetic comp.	mag
94.	TM	Total magnetic component	mag
97.	IPRB	Inclination of probe	mag

Temperature

41.	VTEMP	Voltage	mV
42.	ITEMP	Current	mV
98.	TEMPPT_C	Temperature	deg C
99.	DTEMPPT	Temperature gradient	deg C/km

Complex Resistivity

113.	RES_CR	Resistivity	ohm m
114.	IP_CR	Phase	milliradians
115.	THD1	Total harmonic distortion	
116.	THD2	Harmonic distortion - 2f	
117.	THD3	Harmonic distortion - 3f	
118.	SPV_CR	Self potential	mV
140.	WGTPSULF	Estimate of percent sulfides, from resistivity and phase	weight percent

Lithology, from J. Hulen

101.	SS	Sandstone
102.	SS+LS	Interstratified sandstone and carbonate
103.	CONGLOM	Conglomerate
104.	TUFFFALL	Fallout tuff
105.	SILTTUFF	Silty sandstone and/or tuff
106.	POLYBR	Polymict breccia
107.	ASHFTUFF	Ash-flow tuff
108.	MONOBR	Monomict breccia

Observable core parameters, from J. Hulen, U. of Utah Research Institute

109.	GRAINLO	Grain size, minimum of range
110.	GRAINHI	Grain size, maximum of range
111.	ALTERA	Alteration; weak (1), medium (2), strong (3)
112.	PYRITE	Pyrite; none (0), present (1)
120.	FRACINT	Fracture intensity; none(0), weak (1), medium(2), strong(3). CCM-2 only

Lithology, from D. Larsen, U. of New Mexico

127.	ASHFLOW	Ash-flow tuff
128.	FALLOUT	Fall-out tuff
129.	EPIBREC	Epiclastic breccia
130.	ROCKFALL	Rockfall block (CCM-2 only)
131.	MARGIN	Alluvial/Lake margin strata
132.	DEBRISFL	Sub-lacustrine debris-flow strata
143.	MBXDS	Megabreccia, densely silicified (CCM-1 only)
144.	MBXP	Megabreccia, porous (CCM-1 only)
145.	MBXMS	Megabreccia, moderately silicified (CCM-1 only)
134.	CALCLAM	Calcite Laminations

Laboratory measurements on core samples

125. MS_CORE	Magnetic susceptiblity, R. Reynolds	ucgs
126. MS_COR_L	Magnetic susceptiblity, R. Reynolds	ucgs
139. RHODECKR	Bulk density, E. Decker	g/cc
148. PERMCONC	Permeability, J. Conca	log10(cm/s)
149. PORCONCA	Porosity, J. Conca	percent

X-ray diffraction measurements, from D. Finkelstein, U. of Illinois

2.	GCLAY	Clay	weight percent of solids
3.	GQUARTZ	Quartz	weight percent of solids
7.	GKSPAR	K-feldspar	weight percent of solids
14.	GCALC	Calcite	weight percent of solids
15.	GCLINO	Clinoptilolite	weight percent of solids
44.	GPLAG	Plagioclase	weight percent of solids
30.	GDMIN	Grain density, calc. from mineralogy.	g/cc